

Tomas Binar ✉  
Simona Vasikova  
Pavel Safl  
Jaroslav Talar  
Robert Kutil

<https://doi.org/10.21278/TOF.474047622>

ISSN 1333-1124

eISSN1849-1391

## EVALUATION OF 3D PRINTING USE FOR MULTINATIONAL ARMED FORCES LOGISTIC PROCESSES IN CRISIS SITUATIONS

### Summary

3D printing technology could be an option for the delivery of spare parts in a multinational army supply process, especially in crisis situations, when specific spare parts need to be available as soon as possible. The article deals with the selection of fused filament fabrication as an appropriate method for that purpose by comparing its advantages and disadvantages, as well as the best material (Nylon CF15 Carbon) based on important mechanical properties using the comparative and Saaty's methods. Several samples were made to be exposed to UV radiation in a climate chamber (Q-LAB Q-SUN-Xe3 equipped with a DAYLIGHT-Q filter) and tested according to the ASTM D2565 and ASTM D4459 standards. To compare the mechanical properties of the samples exposed to UV radiation with those of the unexposed ones, a tensile test was done according to the CSN EN ISO 527-2 standard. Finally, the specific spare part was designed and 3D printed, and the delivery times of the standard supply period were compared with those of the 3D printing technology.

*Key words:* 3D printing, Fused deposition modelling, UV radiation of plastics, climate chamber testing, Saaty's method

### 1. Introduction

Nowadays, there is a trend of multinational cooperation in the operations of armed forces. In the North Atlantic Treaty Organization (NATO), individual member states closely cooperate in many foreign military operations, humanitarian actions and exercises, which is closely related to the cooperation in supply processes. The Czech Armed Forces make no exception because behind every operation carried out in the domestic area, there are many supporting activities requiring multinational cooperation. In particular, the use of a multinational supply chain is a very time-consuming process, because its preparation, approval and actual implementation, consisting mainly of transport, storage, transfers, maintenance of material and servicing of equipment, require very careful execution. Therefore, the supply process is economically a very demanding process, not only on the territory of the given state, but also abroad. The place of operation, distance, methods of transport, information and communication systems, as well as the climate, also play an important role here [1-3].

As for individual delivery requests, they are often included in supply cycles, so a specific delivery can be more or less delayed. At the same time, there may be problems with spare parts for a piece of equipment that are not available anywhere for any reason, and thus the piece of equipment becomes irreparable or inoperable and has to be replaced by another one, which further increases costs. For these reasons, efforts are made today to modernize the supply system, which is made possible by the rapid development of modern technologies [3-8].

Undoubtedly, one example of facilitating the supply chain is 3D printing technology, which offers the opportunity to print parts, components, equipment and armament accessories, and other necessary objects for quick temporary repairs of equipment right on the spot. 3D printing technology is now a commonly used technology for the production of spare parts for industrial machines, cars, and aircraft, as well as for the fabrication of small spare parts for households, office equipment, and various special components. It is a modern technology of additive manufacturing that is based on transferring a digital 3D model into a real three-dimensional model by layering the material successively, one layer on top of the other. This concept offers a wide portfolio of various types of printers and types of material, depending on the price and the desired quality of the final product [3], [9-15].

## 2. Materials and methods

This article describes a 3D printing experiment including a specific control element of a remote-controlled weapon station for a 30 mm cannon (RCWS-30). The system is used in the Czech Army Forces on Pandur vehicles as a mounted weapon (Fig. 1). The biggest problem is that the very expensive control panel and its control buttons are not commonly available; therefore, it is not possible to consider them as standard replacement parts. Thus, in the case of damage to or loss of any control button or an element of the controller, it is usually necessary to buy the entire control panel, which costs around 60 thousand EUR, or have this part made to order, which increases costs and delivery time as well [3].



**Fig. 1** RCWS-30 weapon carriage

On the other hand, the control buttons can be easily replaced with non-original pieces, which could be made easily by a 3D printer. This would save time and money, as it would be sufficient to use a minimum of material, and the spare part would be created on the spot within a few minutes. A joystick of the control system with a particular spare part is shown in Fig. 2. The arrow here is a component that was modelled in the SolidWorks program in the design part and then goes through the entire experiment [3], [11-15].



**Fig. 2** RCWS-30 scope controls

In addition, it has to be said that the economics and time evaluation of this experiment are related to a specific spare part and the results were obtained only from the prices of devices and materials at the given time. The project does not deal with the prices of maintenance, energy consumption, the creation of specialized workplaces, or the transport of the 3D printer to the destination or its service. It focuses only on comparing the effectiveness in terms of the time to obtain the required part, which is the most important parameter for restoring the function of the given device, especially in cases of emergency [3], [11-15].

## 2.1 3D printing technologies considered in the project

Three best-known 3D printing technologies were considered for the control element production, from which the best variant for the given purpose was subsequently selected [11]:

- Stereolithography (SLA) - a method using a base material in the form of a liquid photopolymer resin that can be cured by UV light.
- Selective Laser Sintering (SLS) - a technology which uses a powder-based material (both plastics and metals), which is joined layer by layer by melting while a powerful laser is used.
- Fused Filament Fabrication (FFF) - a method that, in order to create 3D objects, uses the melting of a plastic filament in a string that is unrolled from a storage coil and then passes through a nozzle, and individual layers are formed. This method is a derivative of the commonly known Fused Deposition Modelling (FDM), which is a registered patent of the Stratasys company [16].

## 2.2 Selection of the right method

Based on the possibilities and a simple comparison of the advantages (Table 1) and disadvantages (Table 2) of the above-mentioned methods, the most advantageous variant was selected for the experiment, especially in terms of the complexity of the implementation and the costs [3], [16], [17].

**Table 1** Advantages of selected 3D printing technologies

SLA	SLS	FFF
High accuracy	No support needed	Cheaper and more accessible
High-quality printing of complex shapes	Sintering of defined sections only	Safe and cheap material
Possibility of serial production	Easy recycling of unused material	Simple to use
Special components printing	Good product durability	Various types of material for universal use
		No need to use a protective equipment

**Table 2** Disadvantages of selected 3D printing technologies

SLA	SLS	FFF
High acquisition costs	High acquisition costs	Lower accuracy
High material costs	High material costs	Necessity of mechanical processing of the final model
Printing time depends on the complexity of the object	Costly and complex cleaning of the machine from powder	Limited life of the material
The smell of a resin	Low material variability	Poor regulation of the material layer
It is necessary to avoid contact of the material with sunlight	Risk of material shrinkage and model unevenness	
Necessity to use PPE		
Necessity of soaking the final product in isopropylalcohol		
Necessity of mechanical removal of excess material with the risk of damaging the model		
It is necessary to replace the resin container at certain intervals		

Based on the established facts, the use of the FFF method was most suitable for our purposes. It is simple and affordable for almost every consumer, has a huge range of different materials and is safe to use. For these reasons, this technology was used for the printing of test samples from the selected material [3].

### 2.3 Materials and methods

For this experiment, a commonly available 3D printer, Ender 3 Pro, based on FFF technology, was chosen, together with the most commonly purchased printing filaments on the market (PET-G, ASA-Extrafill, Nylon CF15 Carbon, PLA Crystal Clear and ABS-Extrafill). Based on a comparison of essential mechanical properties, the most suitable material for 3D printing was subsequently selected. To verify the properties of this material in service, it was

tested under UV radiation in the Q-LAB Q-SUN-Xe3 climatic chamber and also mechanically by tension using the TEMPOS ZD20/200 kN universal tensile testing machine. The resistance of the material to UV radiation was verified using a tensile test by comparing the values of samples unexposed to UV radiation with the values of samples exposed to UV radiation. SolidWorks and Ultimaker Cura software packages were used in the design of a specific control element model [18-24].

### 3. Results and discussion

#### 3.1 Selection of a suitable material

For 3D printing using the FFF method, first, it was necessary to select the most suitable material. The selection of a suitable material was made on the basis of the selected mechanical properties of the available materials (tensile strength, elongation after a break, modulus of elasticity in tension, and material density). The properties of the materials were first considered based on a simple comparison and then the selection was made using Saaty's method [25-28].

##### 3.1.1 Comparison of the material properties

An overview of selected mechanical properties (criteria C<sub>1</sub>-C<sub>4</sub>) of available material variants (V<sub>1</sub>-V<sub>5</sub>) is shown in Table 3; the table enables a direct comparison of the properties [25-27].

**Table 3** Selected properties of the given material variants

Selected property	PET-G (V <sub>1</sub> )	ASA Extrafill (V <sub>2</sub> )	Nylon CF15 Carbon (V <sub>3</sub> )	PLA Crystal Clear (V <sub>4</sub> )	ABS Extrafill (V <sub>5</sub> )
Tensile strength [MPa] (C <sub>1</sub> )	50	40	54.5	50	39
Elongation after breaking [%] (C <sub>2</sub> )	20	35	3	5	20
Modulus of elasticity in tension [MPa] (C <sub>3</sub> )	2100	1726	500	3500	2200
Material density [g·cm <sup>-3</sup> ] (C <sub>4</sub> )	1.27	1.07	1.08	1.24	1.04

As it is clear from the table above, Nylon CF15 Carbon (V<sub>3</sub>) is the material with the highest tensile strength (54.5 MPa). On the other hand, this material has the lowest (3%) elongation of the given materials, which is related to the lowest modulus of elasticity (500 MPa), indicating the highest stiffness of the selected materials. PET-G (V<sub>1</sub>) and ABS (V<sub>5</sub>) are more flexible than Nylon CF15 Carbon (V<sub>3</sub>) and ASA Extrafill (V<sub>2</sub>), and PLA Crystal Clear (V<sub>4</sub>) is the best in this area. Based on the strength and stiffness values of the material, it is possible to select the material depending on the final use of the given product. For our purposes, a rigid material was more suitable than a flexible one, and therefore higher stiffness values were preferred. The density of the material is closely related to the weight of the final model; in our case, the density values of the selected materials were almost the same, with the exception of PET-G (V<sub>1</sub>) and PLA Crystal Clear (V<sub>4</sub>), which show slightly higher values [3], [25], [26].

### 3.1.2 Saaty's method

For Saaty's method, the same variants of the material (V<sub>1</sub>-V<sub>5</sub>) were considered [26-28]:

- V<sub>1</sub> - PET-G
- V<sub>2</sub> - ASA Extrafill
- V<sub>3</sub> - Nylon CF15 Carbon
- V<sub>4</sub> - PLA Crystal Clear
- V<sub>5</sub> - ABS Extrafill

To select a suitable material that will be durable and that can be efficiently produced, four criteria specified in Table 3 (C<sub>1</sub>-C<sub>4</sub>) are considered [26-28]:

- C<sub>1</sub> - Tensile strength [MPa]
- C<sub>2</sub> - Elongation after breaking [%]
- C<sub>3</sub> - Modulus of elasticity in tension [MPa]
- C<sub>4</sub> - Material density [g·cm<sup>-3</sup>]

According to Saaty's method, importance weights are determined for individual criteria. These weights are shown in Table 5, and the values are based on auxiliary table no. 1 - Table 4 [28].

**Table 4** Auxiliary table no. 1 for Saaty's method

Importance of the criteria	Score points if the statement is true	Score points if the statement is not true
Both compared criteria are equally important	1	1
The criterion in the line is slightly more important	3	1/3
The criterion in the line is even more important	5	1/5
The criterion in the line is much more important	7	1/7
The criterion in the line is extremely more important	9	1/9

The weights are calculated according to the expression (1) given below [28]:

$$v_i = \frac{G_i}{\sum_{i=1}^n G_i} \tag{1}$$

where  $G_i$  is the geometric mean.

**Table 5** Saaty's table of individual variant evaluation

Criterion	C <sub>1</sub>	C <sub>2</sub>	C <sub>3</sub>	C <sub>4</sub>	Geometric mean	Total weight
C <sub>1</sub>	1	5	3	5	2.9428	0.4958
C <sub>2</sub>	1/5	1	1/7	1/5	0.2749	0.0463
C <sub>3</sub>	1/3	7	1	7	2.1407	0.3606
C <sub>4</sub>	1/5	5	1/9	1	0.5774	0.0973
Total					5.9358	

An expert determination of partial evaluations is performed on the basis of a linear function (2). This method is suitable for evaluating multi-criteria variants. Its biggest advantage is that quantitative and qualitative criteria can be compared. Table 6 shows individual criteria (C<sub>1</sub>-C<sub>4</sub>) and specific values for each of the variants, including the measurement units in which the criterion is calculated. This is an auxiliary table no. 2 needed for the actual calculation of the most suitable variant (V<sub>1</sub>-V<sub>5</sub>) using this method [26], [28].

**Table 6** Auxiliary table no. 2 for the best variant evaluation

Selected criterion	Measurement unit	Individual variants of the selected materials				
		V <sub>1</sub>	V <sub>2</sub>	V <sub>3</sub>	V <sub>4</sub>	V <sub>5</sub>
C <sub>1</sub>	MPa	50	40	54.5	50	39
C <sub>2</sub>	%	20	35	3	5	20
C <sub>3</sub>	MPa	2100	1726	500	3500	2200
C <sub>4</sub>	g·cm <sup>-3</sup>	1.27	1.07	1.08	1.24	1.04

The overall rating of the selected variants is calculated according to (2) [21-23].

$$H^j = \sum_{i=1}^n v_i \cdot h_i^j \tag{2}$$

where  $H_j$  is the overall evaluation of the  $j^{\text{th}}$  variant,  $v_i$  is the weight of the  $i^{\text{th}}$  criterion,  $n$  is the number of evaluated criteria, and  $h_i^j$  is the partial evaluation of the  $j^{\text{th}}$  variant with respect to the  $i^{\text{th}}$  criterion, which is calculated according to (3) [26], [28].

$$h_i^j = \frac{x_i^j - x_i^0}{x_i^1 - x_i^0} \tag{3}$$

where  $x_i^j$  is the value of the  $i^{\text{th}}$  criterion of the  $j^{\text{th}}$  variant,  $x_i^1$  is the best value among all variants of the  $i^{\text{th}}$  criterion (considering quantitative criteria, the assigned value is 1),  $x_i^0$  is the worst value among all variants of the  $i^{\text{th}}$  criterion (considering quantitative criteria, the assigned value is 0) [26], [28].

Table 7 shows the criteria and selected variants. The weight values of the criteria, which were obtained using Saaty's method in the previous case (Table 6), are also included. The final ranking is determined starting from the highest calculated  $H^j$  values to the lowest [26], [28].

**Table 7** Calculation of the most suitable variant

Criterion	Weight $v_i$	The worst value	The best value	Selected variants $h_i^j$				
				V <sub>1</sub>	V <sub>2</sub>	V <sub>3</sub>	V <sub>4</sub>	V <sub>5</sub>
C <sub>1</sub>	0.4958	39	54.5	0.71	0.06	1	0.71	0
C <sub>2</sub>	0.0463	35	3	0.47	0	1	0.94	0.47
C <sub>3</sub>	0.3606	3500	500	0.47	0.59	1	0	0.43
C <sub>4</sub>	0.0973	1.27	1.04	0	0.87	0.83	0.13	1
Overall evaluation of $H_j$ (2)				0.5433	0.3271	0.9835	0.4082	0.2741
The final rankings				2	4	1	3	5

The variant with the highest overall ranking is taken as the best. In this case, it is variant 3 (Nylon CF15 Carbon material) with a total score of 0.9835. This material was further subjected to tests in a climatic chamber, and tensile tests were done to determine its resistance [3], [28].

### 3.2 Testing of the selected material

A total of sixteen test samples of the given shape (Fig. 3) and dimensions (Table 8) were created from the selected material, Nylon CF15 Carbon, according to the CSN EN ISO 527-2 standard, type 1A [24]. Subsequently, UV testing was carried out on the samples in a climatic chamber, and a tensile test was done to verify the mechanical properties and applicability of the material in indoor and outdoor conditions [3], [23], [29].

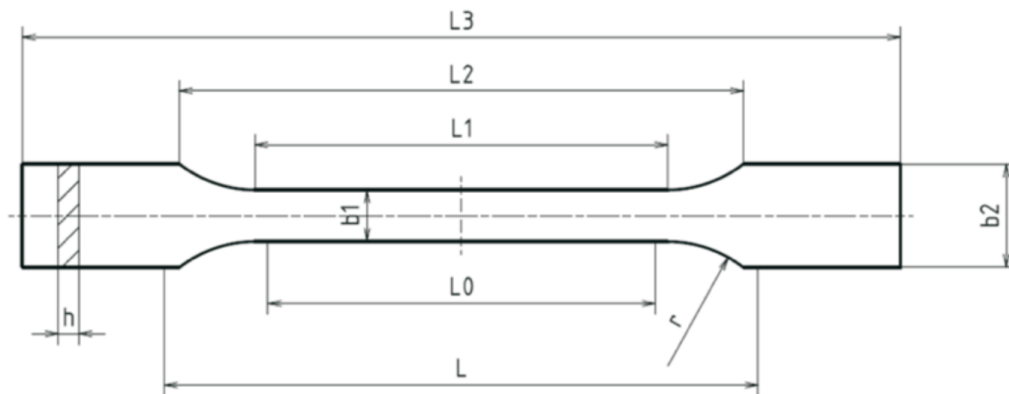


**Fig. 3** The shape and dimensions of a test sample [29]

**Table 8** Dimensions of the test sample [29]

Dimension	Parameter	Value of the parameter [mm]
L3	Total length	170
L1	The length of the tapered part with parallel edges	$80 \pm 2$
R	Radius	$24 \pm 1$
L2	The distance between flared parts with parallel edges	$109.3 \pm 3.2$
b2	The width of the ends	$20 \pm 0.2$
b1	The width of the tapered part	$10 \pm 0.2$
h	Recommended thickness	$4 \pm 0.2$
L0	Initial measured length	$75 \pm 0.5$
L	Initial distance between jaws	$115 \pm 1$

### 3.2.1 Climatic chamber testing

For the experiment, a Q-SUN-Xe3 type climate chamber from Q-LAB was used. This chamber meets the ASTM D2565 and ASTM D4459 standards, and the samples could be tested there for both outdoor and indoor uses. There were three xenon lamps in the climate chamber that could simulate different types of solar radiation using different types of filters. In our case, the DAYLIGHT-Q filter type was used, which is intended for the simulation of midday light in the summer, while its properties correspond most closely to reality. For the evaluation, twelve samples were tested in three cycles (Table 9). The radiation power was set to  $50 \text{ W/m}^2$  [24].

**Table 9** Parameters of UV radiation cycles in the climate chamber

UV cycle	Testing time [hours]
UV 1	192
UV 2	384
UV 3	768

After the total time of exposure to UV radiation, which was 32 days (768 hours), the test samples did not show any visible signs of wear, the colour remained the same, and there was no distortion of the samples (Fig. 4). It follows that this could be a suitable material for the given purpose.



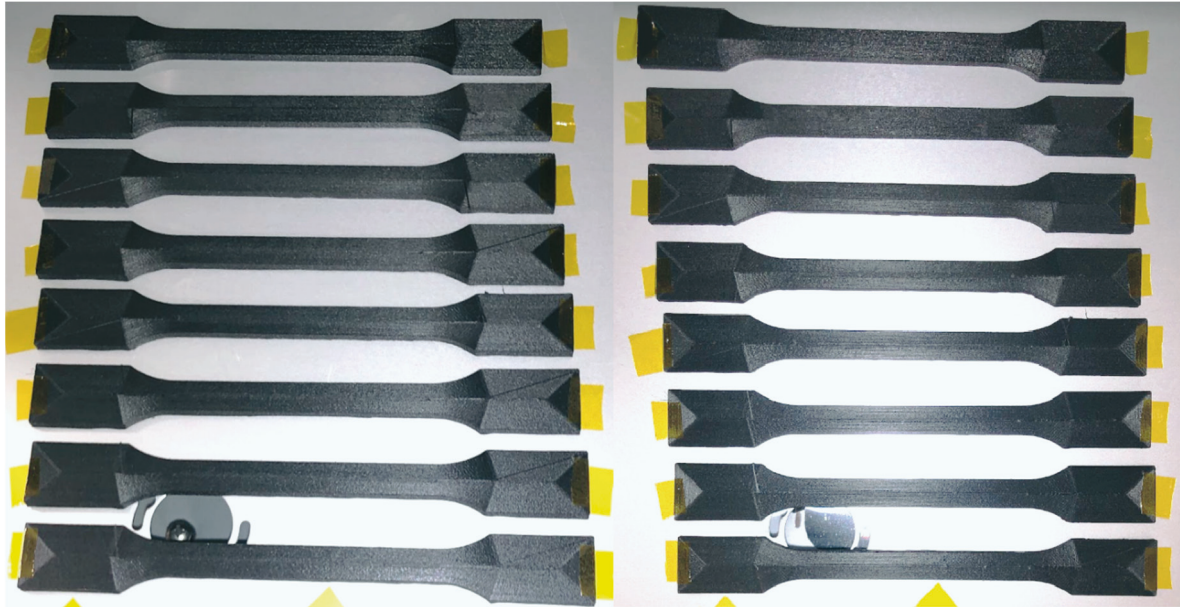


**Fig. 4** The test samples after exposure to UV radiation in a climatic chamber

### 3.2.2 Tensile testing

To verify the mechanical properties of the material, a tensile test was also performed on the samples. First, the tensile test was performed on the samples that did not go through the climate chamber process (without UV), and then on the samples that were tested in 3 cycles of exposure to UV radiation. The samples tested in the climatic chamber are divided according to the time cycles of extraction from the chamber (UV1, UV2, and UV3). Table 10 shows the average values of individual samples that underwent the tensile test at the average measured force.

**Table 10** Average values of tensile test carried out on test samples

UV cycle	Time, $t$ [s]	Lengthening, $s$ [mm]	Max. force, $F_{max}$ [N]	Stress at the yield point [MPa]	Proportional lengthening [%]
Without UV	49.05	4.23	5 274.64	131.12	5.26
UV1	42.68	3.63	5 204.41	130.86	4.54
UV2	42.04	3.58	5 162.44	129.06	4.47
UV3	34.50	2.89	4 853.34	121.33	3.63

From the results of tensile test shown in Table 10, one can see that the material exposed to UV radiation showed lower values of elongation when stretched than the material that was not exposed to climatic conditions. Also, one can see that the radiation did not have a significant effect on the strength, and that the strongest effect was noted in the relative elongation. Therefore, it can be concluded that longer exposure to UV radiation results in a more brittle material with decreased elasticity (in our case, by almost half). However, changes in the material due to these adverse effects do not affect the quality of the material required for the functioning of the part, and thus the material is considered to be appropriate for the purpose. Figure 5 shows the damage to the samples after the tensile test.

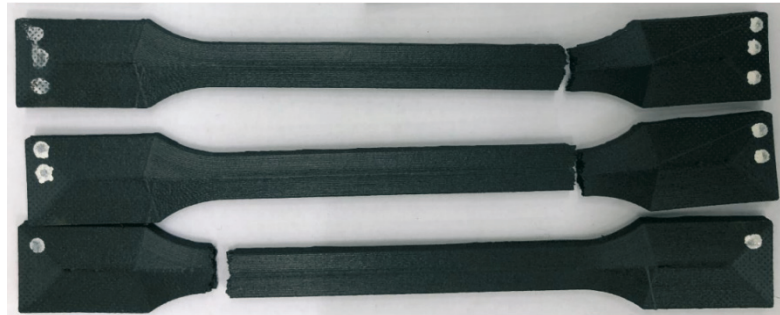


**Fig. 5** Damaged samples after the tensile test

### 3.3 The process of acquiring the data for the 3D printing of the control part

After successful testing of the material, it was possible to start the process of design and creation of the sight control element for a remote-controlled weapon station, RCWS-30, using 3D printing technology; the process had four stages. To speed up and simplify the process, it was assumed to create a new part based on the part removed from another RCWS-30.

#### 3.3.1 Stage 1

In the first stage, the object was created by measuring dimensions and shapes that could be processed in the SolidWorks software (Fig. 6) in about 30 minutes.

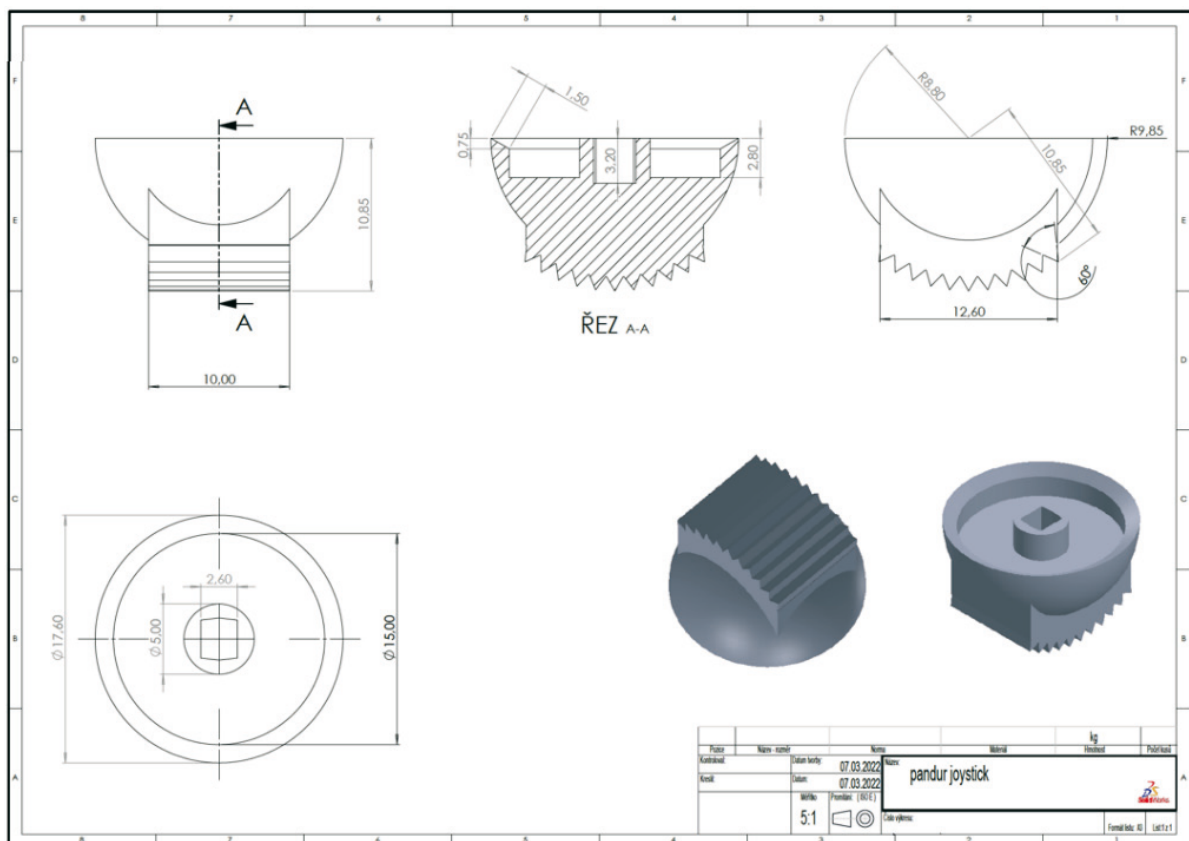


**Fig. 6** A drawing and a 3D model of the control in SolidWorks software

For the sake of interest, it can be mentioned that scanning the element using a 3D scanner (Figs. 7 and 8) can serve as an alternative, which is especially suitable for more complex shapes. In addition, scanning speeds up the whole process even more, although it may be only by a few minutes. However, it is not always available.

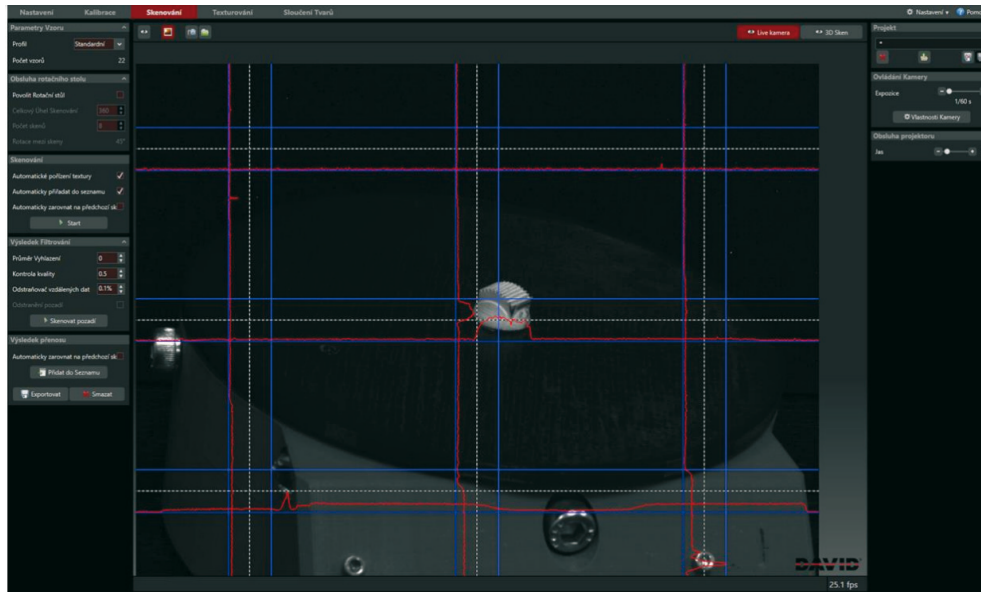


Fig. 7 Scanning of the control element using a 3D scanner

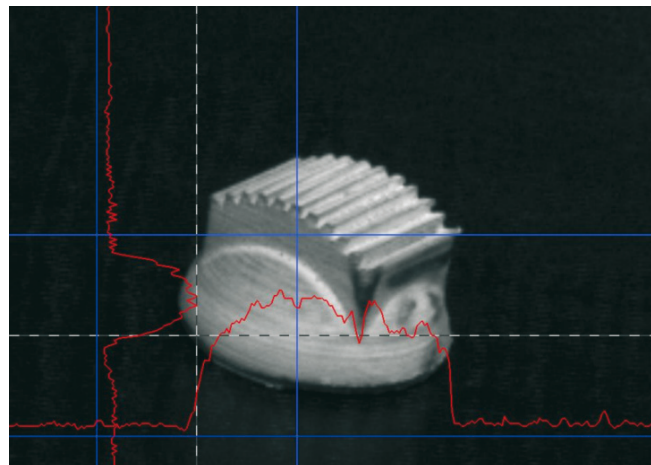


Fig. 8 Enlarged scanned control element

### 3.3.2 Stage 2

The second stage involved converting the modelled object into an STL format for a 3D printer (Fig. 9). The file in STL format contained a modelled object with a description of its surface geometry in 3D format, which could be viewed from all sides; it was also used to prepare the model for subsequent printing and data transfer to a 3D printer. The conversion to STL format itself took 30 seconds. The low-resolution STL format of the file was chosen because its resolution was in accordance with 3D printing accuracy.

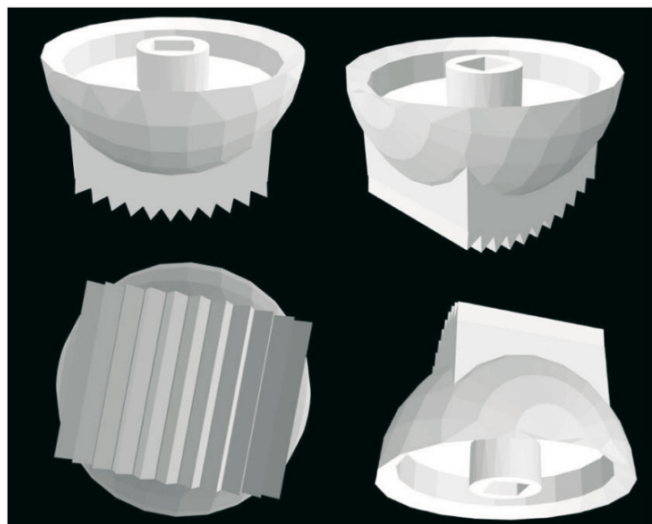
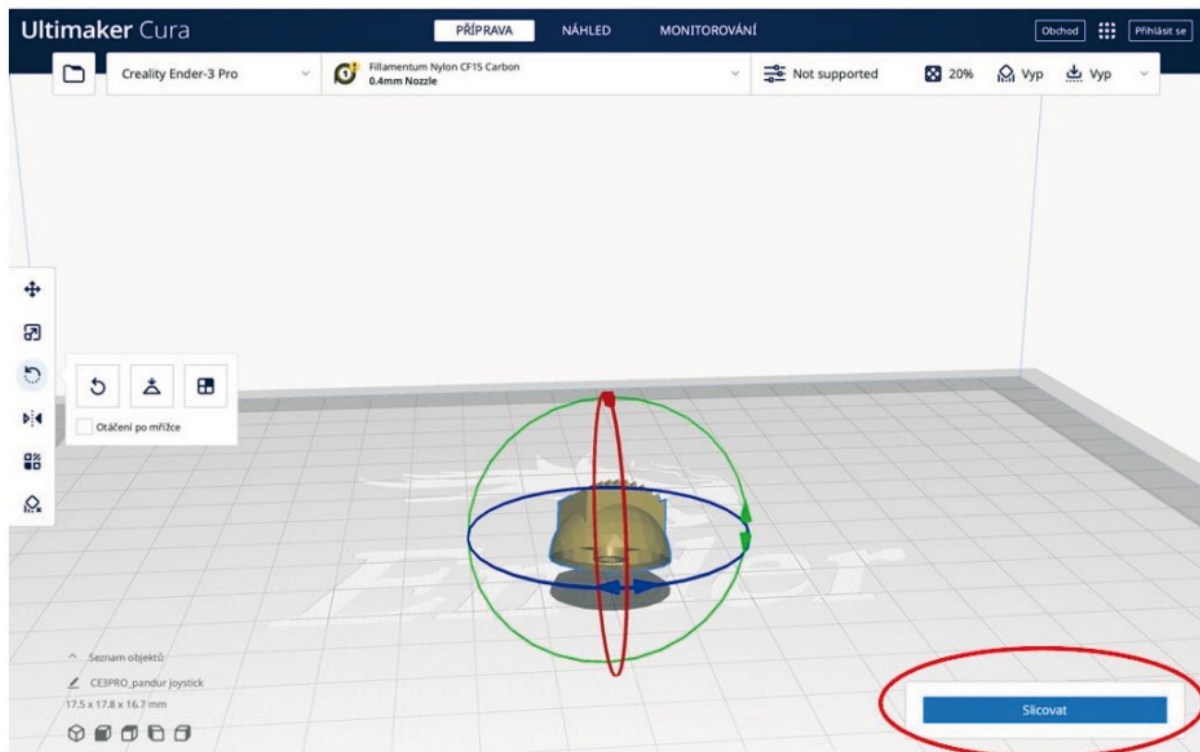


Fig. 9 Converted object to STL format for a 3D printer

### 3.3.3 Stage 3

The third stage was characterized by the conversion of the file in STL format to the CURA slicer, where a G-Code was created based on printing parameters. The preparation mainly consisted of comparing the dimensions and cutting the given 3D model into layers for 3D printing. In the Ultimaker Cura software (Fig. 10), it is also possible to preset the type of printing material, and the slicer will subsequently generate all the necessary information (temperature of the plate and extruder, height of the printed layer, etc.). Importing the STL file into the slicer and converting it to G-Code took 2 minutes.



**Fig. 10** Data preparation and conversion to G-Code in the Ultimaker Cura software

### 3.3.4 Stage 4

In the final, fourth stage, the model was transferred to the 3D printer, where the actual printing began. It took 8 minutes to print the whole control button (Fig. 11). After printing the control button, it would be possible to immediately place the control device into the weapon system and reactivate it.



**Fig. 11** The printed control button, ready to be used

### 3.4 Time analysis of spare part delivery

Now, we should evaluate the time of a standard supply cycle in comparison with the new 3D printing possibilities. The time data for the current standard supply method are shown in Table 11, while the data for the 3D printing of a specific spare part are shown in Table 12.

**Table 11** Delivery times of the current supply method

Standard material acquiring order	Process	Time (weeks)	Time (hours)
1	Operational logistics support planning	2	336
2	Approval process	2	336
3	Acquisition activity	8	1344
4	Delivery of material in a stock	2	336
5	Transport to required destination	6	1008
Total time		20	3360

From Table 11, it is clear that the process of acquiring goods using the current method of supply and subsequent transportation to the area of operation is very time-consuming. Since it is not possible to transport only one thing in this way, several requirements must first come together. Only after their approval can the necessary goods and material be transported to the destination. In addition, in crisis situations, there are other factors delaying the delivery. For clarity, the delivery process is divided into 5 stages, which are calculated for a total of 3360 hours. However, for the reasons mentioned above, this is not a fixed time figure but variable, depending on various circumstances that are part of the process.

Table 12 shows the stage of the process when 3D technology was used for a specific selected part. The time data are variable, depending on the size and complexity of the printed object, the required quality, speed of printing, etc. When compared, the data in Tables 11 and 12 show the difference in time between the classic acquisition and the 3D printing of the desired spare part.

**Table 12** A new way of supplying the part with 3D printing

Material acquiring order with 3D printing	Process	Time (min)	Time (hours)
1	Drawing and 3D model creating (CAD)	30	0.500
2	Converting to STL	0.5	0.008
3	G-Code processing	2	0.034
4	3D printing at the required destination	8	0.133
Total time		40.5	0.675

### 3.5 Acquisition costs of 3D printing

When considering the possibility of acquiring 3D printing technology, it is necessary to calculate the costs. Due to the expensive and relatively long supply cycles, the acquisition costs of 3D printing are relatively negligible (Table 13). In our case, the acquisition costs were only about €244 with the acquisition of the printer included; without it, the price would have been much lower. From the point of today's prices of fuel and lubricants, service and maintenance of the vehicle fleet, and wages of workers, it is clear that this is really a negligible cost. The final prices will, of course, depend on the number of 3D printers purchased, their types, and the quality of the material used, depending on the size and required quality of the parts to be 3D printed.

**Table 13** Approximate acquisition costs of basic 3D printing technology

Acquisition of 3D printing technology	Price (EUR)
SolidWorks software (cost of 0.5 hour of drawing, calculated from SolidWorks Annual Subscription)	0.075
Ultimaker Cura software	0 (free to download)
Price of the Creality Ender 3 Pro 3D printing machine	243.000
Average printer costs of 8 minutes of printing (electricity, etc.)	0.009
Nylon CF15 Carbon printing wire for 1 spare part	0.598
Total price (3D printer acquisition price included)	243.682
Total price (with average printer costs of 8 minute printing only)	0.682

## 4. Conclusion

Multinational logistics processes are very complex and lengthy, so they require very careful preparation and professional staff. This process can be optimized thanks to modern technologies. 3D technologies are now commonly used in companies and households thanks to their relatively low demands and prices, and their use is also considered in army supply processes.

For our purpose, the classic, most widespread method of 3D printing (FFF) was quite sufficient. Based on market research, the five most widely used materials were determined and subsequently compared and evaluated according to their mechanical properties. Nylon CF15 Carbon with carbon fibres was chosen as the most suitable material as it is very durable thanks to its mechanical properties. Test samples were created from this material, which were subjected to UV radiation in a climate chamber to verify the properties of the material in indoor and outdoor conditions. Mechanical properties of the material were verified in a tensile test performed on the samples that had not been exposed to UV radiation and those exposed to UV radiation. The obtained data showed that exposure to UV radiation had a certain effect on the mechanical properties of the given material. As the time of exposure to UV radiation increased, the fragility of the material increased and its elasticity decreased. This was particularly evident from the results of the relative elongation of the material, while all monitored parameters had a decreasing character. After the testing, the design of the selected component proceeded.

In the experiment, it was assumed that when using the possibility of manufacturing components using 3D technology, the entire 3D printer with all components and the responsible person would be immediately transported to the operation area at the designated workplace. Based on the requirements and the necessary information, the 3D printer would then be able to print the missing component in a few minutes right on the spot. This would save a lot of time with respect to the time required for a new part to be custom made or a new control system delivered. This is very beneficial, especially in crisis situations, when there is no time or material to spare, and despite the very good level of cooperation of individual NATO army units, this simple modernization offers an additional possibility of quick and flexible reactions to unexpected situations and problems.

### Acknowledgement

The study was supported by the Ministry of Defence of the Czech Republic projects No. DZRO K-109 and No. OFVVU20140001. This research was carried out in the Centre for Research and Utilization of Renewable Energy (CVVOZE). The authors gratefully acknowledge the financial support from the Ministry of Education, Youth and Sports of the Czech Republic under the NPU I Programme (project No. LO1210).

The study was also supported by the specific graduate research of the Brno University of Technology No. FEKT-S-14-2293.

### REFERENCES

- [1] AJP-4 ALLIED JOINT DOCTRINE FOR LOGISTICS: NATO STANDARDIZATION OFFICE (NSO), **2018**. <https://www.handbook.cimic-coe.org/8.-annex/reference-docs/ajp-3.19-eda-v1-e.pdf>
- [2] EU CONCEPT FOR RECEPTION, STAGING, ONWARD MOVEMENT & INTEGRATION (RSOI) FOR EU-LED MILITARY OPERATIONS. Brusel, COUNCIL OF THE EUROPEAN UNION, **2012**. <https://data.consilium.europa.eu/doc/document/ST-9844-2012-INIT/en/pdf>
- [3] Kubackova, K. Use of new technologies for the supply system. Master thesis. University of Defence, Faculty of Military Leadership, Department of Logistics. Brno, 2022.
- [4] Na'amnh, S.; Husti, I.; Daroczi, M. Implementing the augmented reality as an Industry 4.0 application to simplify the busbar bending process during the Covid-19 pandemic. *Transactions of Famena* **2021**, 45(3), 115-125. <https://doi.org/10.21278/TOF.453026921>
- [5] Zoubek, M.; Poor, P.; Broum, T.; Simon, M. Methodology proposal for storage rationalization by Implementing Principles of Industry 4.0. In a technology-driven warehouse. *Transactions of Famena* **2021**, 44(4), 75- 98. <https://doi.org/10.21278/TOF.444016220>
- [6] Mahalingam, S.; Babu, A., S. Experimental Study on Woven Ramie Fibre Epoxy Composite with Silane-Treated Groundnut shell Powder as a Filler Material. *Transactions of Famena* **2023**, 47(1), 1-12. <https://doi.org/10.21278/TOF.471048622>
- [7] Sivakumar, A.; Saravanakumar, S.; Sathiamurthi, P.; Karthivinit, K., S. Forecasting the equipment effectiveness in total productive maintenance using an intelligent hybrid conceptual model. *Transactions of Famena* **2022**, 46(3), 29-40. <https://doi.org/10.21278/TOF.463042822>
- [8] Trstenjak, M.; Opetuk, T. Industry 4.0 readiness factor calculation and process planning: State-of-the-art review. *Transactions of Famena* **2020**, 44(3), 1-22. <https://doi.org/10.21278/TOF.44301>
- [9] Kückelhaus, M.; Yee, P.M. 3D printing and the future of supply chains. **2016**. Google Scholar.
- [10] Berman, B. 3-D printing: The new industrial revolution. *Bus. Horiz.* **2012**, 55(2), 155-162. <https://doi.org/10.1016/j.bushor.2011.11.003>
- [11] Westerweel, B.; Basten, R.; den Boer, J.; van Houtum, G.J. Printing Spare Parts at Remote Locations: Fulfilling the Promise of Additive Manufacturing. *Prod OperManag.* **2021**, 30, 1615-1632. <https://doi.org/10.1111/poms.13298>
- [12] Holmström, J.; Partanen, J.; Tuomi, J.; Walter, M. Rapid manufacturing in the spare parts supply chain: Alternative approaches to capacity deployment. *J. Manuf. Technol. Manag.* **2010**, 21(6), 687-697. <https://doi.org/10.1108/17410381011063996>
- [13] Khajavi, S.H.; Partanen, J.; Holmström, J. Additive manufacturing in the spare parts supply chain. *Comput. Ind.* **2014**, 65(1), 50-63. <https://doi.org/10.1016/j.compind.2013.07.008>

- [14] Jaksic, M.;Trkman, P. (2018). 3D Printing as an Alternative Supply Option in Spare Parts Inventory Management. *Operations Research Proceedings 2016* **2017**, Springer.  
[https://doi.org/10.1007/978-3-319-55702-1\\_81](https://doi.org/10.1007/978-3-319-55702-1_81)
- [15] Booth, J.; Edwards, E.; Whitley, M.; Kranz, M.; Seif, M.; Ruffin, P. Military comparison of 3D printed vs commercial components. *Nano-, Bio-, Info-TechSensors, and 3D Systems II*, 105970J **2018**.  
<https://doi.org/10.1117/12.2300773>
- [16] 3D printing at a glance. Material for 3D print, Solidify 3D **2023**. <https://www.materialpro3d.cz/3d-tisk-v-kostce/>
- [17] Vujovic, I.; Soda, J.; Kuzmanic I.; Petkovic M. Parameters Evaluation in 3D Spare Parts Printing. *Electronics* **2021**; 10(4), 365. <https://doi.org/10.3390/electronics10040365>
- [18] Guide for Creality ENDER-3.  
<https://dwn.alza.cz/manual/66958+&cd=1&hl=cs&ct=clnk&gl=cz&client=safari>
- [19] Datasheet - PLA CrystalClear. Material and accessories for 3D print, Fillamentum.  
[https://www.materialpro3d.cz/user/related\\_files/technical\\_data\\_sheet\\_pla\\_crystal\\_clear.pdf](https://www.materialpro3d.cz/user/related_files/technical_data_sheet_pla_crystal_clear.pdf)
- [20] Datasheet - PET-G. Material and accessories for 3D print, Fillamentum.  
[https://www.materialpro3d.cz/user/related\\_files/technical-datasheet\\_petg\\_en\\_06052020\\_fe.pdf](https://www.materialpro3d.cz/user/related_files/technical-datasheet_petg_en_06052020_fe.pdf)
- [21] Datasheet - ABS extrafill. Material for 3D print, Fillamentum.  
[https://www.materialpro3d.cz/user/related\\_files/technical\\_data\\_sheet\\_abs\\_extrafill\\_03012019-19.pdf](https://www.materialpro3d.cz/user/related_files/technical_data_sheet_abs_extrafill_03012019-19.pdf)
- [22] Datasheet - ASA Extrafill. Material for 3D print, Fillamentum.  
[https://fillamentum.com/wpcontent/uploads/2020/10/Technical-Data-Sheet\\_ASA-Extrafill\\_03012019.pdf](https://fillamentum.com/wpcontent/uploads/2020/10/Technical-Data-Sheet_ASA-Extrafill_03012019.pdf)
- [23] Datasheet - Nylon CF15 Carbon. Materialfor 3D print, Fillamentum.  
[https://www.materialpro3d.cz/user/related\\_files/technical\\_data\\_sheet\\_nylon\\_cf15\\_carbon\\_03012019.pdf](https://www.materialpro3d.cz/user/related_files/technical_data_sheet_nylon_cf15_carbon_03012019.pdf)
- [24] Q-SUN Prospect. <https://labimexcz.cz/laboratore/produkty/komory-pro-slunecni-simulace-q-lab/qsun-xe-1b-s-bc-bs/>
- [25] Mu, E.; Pereyra-Rojas, M. Practical Decision Making: An Introduction to the Analytic Hierarchy Process (AHP) Using Super Decisions V2. *Springer Briefs in Operations Research*. New York, Springer, **2016**. ISBN 3319338617, 9783319338613
- [26] Varian, H. R. Equity, envy, and efficiency. *Journal of Economic Theory* **1974**, 9(1), 63-91.  
[https://doi.org/10.1016/0022-0531\(74\)90075-1](https://doi.org/10.1016/0022-0531(74)90075-1)
- [27] Eaves, B.C. A finite algorithm for the linear exchange model. *Journal of Mathematical Economics* **1976**, 3(2), 197-203. [https://doi.org/10.1016/0304-4068\(76\)90028-8](https://doi.org/10.1016/0304-4068(76)90028-8)
- [28] Saaty, T. L. Decision making with the analytic network process. *Economic, political, social and technological applications with benefits, opportunities, costs and risks*. New York, Springer, **2013**. ISBN 978-1-4614-7279-7, 1-4614-7279-2.
- [29] CSN EN ISO 527-2 (640604): Plastics - Tensile characteristics, part 2, Testing conditions. Prague: Technical normatives, **2012**.

Submitted: 31.10.2022

Accepted: 11.8.2023

Tomas Binar\*  
Jaroslav Talar  
Robert Kutil  
University of Defence, Faculty of Military  
Leadership, Department of Logistics,  
Brno, Czech Republic  
Simona Vasikova  
Pavel Safl  
Faculty of Electrical Engineering and  
Communication, Brno University of  
Technology, Department of Electrical and  
Electronic Technology,  
Brno, Czech Republic  
\*Corresponding author:  
tomas.binar@unob.cz